the FEBS Journal
REVIEW ARTICLE

Ryanodine receptor calcium release channels: lessons from structure–function studies

Fernando J. Amador, Peter B. Stathopulos, Masahiro Enomoto and Mitsuhiko Ikura

Ontario Cancer Institute and Department of Medical Biophysics, University of Toronto, Canada

Keywords
cryo-electron microscopy; excitation–contraction coupling; inositol 1,4,5-trisphosphate receptor; malignant hyperthermia; nuclear magnetic resonance spectroscopy; ryanodine receptor; X-ray crystallography

Correspondence
M. Ikura, Ontario Cancer Institute and Department of Medical Biophysics, University of Toronto, Ontario M5G 1L7, Canada
Fax: (416) 581-7564
Tel: (416) 581-7550
E-mail: mikura@uhnres.utoronto.ca

(Received 5 December 2012, revised 24 January 2013, accepted 4 February 2013)

doi:10.1111/febs.12194

Ryanodine receptors (RyRs) are the largest known ion channels. They are Ca^{2+} release channels found primarily on the sarcoplasmic reticulum of myocytes. Several hundred mutations in RyRs are associated with skeletal or cardiomyocyte disease in humans. Many of these mutations can now be mapped onto the high resolution structures of individual RyR domains and on full-length tetrameric cryo-electron microscopy structures. A closely related Ca^{2+} release channel, the inositol 1,4,5-trisphospate receptor (IP_3R), shows a conserved structural architecture at the N-terminus, suggesting that both channels evolved from an ancestral unicellular RyR/IP_3R. The functional insights provided by recent structural studies for both channels will aid in the development of rationale treatments for a myriad of Ca^{2+}-signaled malignancies.

Introduction

Ryanodine receptors (RyRs) play a vital role in muscle excitation–contraction (E-C) coupling [1,2]. They release Ca^{2+} from the sarcoplasmic reticulum (SR) into the cytosol, which sets off a cascade of events resulting in muscle contraction. E-C coupling refers to the close interaction between the dihydropyridine receptor (DHPR) L-type Ca^{2+} channels and RyRs (i.e. RyR1 and RyR2), where depolarization of the plasma membrane is coupled to opening of RyRs [3]. Prior to their purification and identification, RyRs were visualized by thin section or negative stain electron microscopy, where they appeared as electron dense regions spanning the intracellular junctions and transverse tubules of striated muscle [4]. Several groups successfully monitored the solubilization, purification and isolation of RyRs from striated muscle using ^{3}H-ryanodine [5–7], a plant alkaloid and a potent insecticide [8]. They showed that RyRs form homotetramers with molecular weights of ~ 2.2 MDa and each monomer consists of ~ 5000 amino acids.

In the same year that RyR1 was cloned, another Ca^{2+} release channel, the inositol 1,4,5-trisphospate receptor (IP_3R), from rat and mouse had its primary structure determined [9,10]. These studies revealed that

Abbreviations
ARVD, arrhythmogenic right ventricular dysplasia; CaM, calmodulin; CCD, central core disease; CPVT, catecholaminergic polymorphic ventricular tachycardia; cryo-EM, cryo-electron microscopy; DHPR, dihydropyridine receptor; E-C, excitation–contraction; GFP, green fluorescent fusion protein; HS, hot spot; IP_3R, inositol 1,4,5-trisphosphate receptor; MH, malignant hyperthermia; NTD, N-terminal domain; R2, spin–spin relaxation rate; RyR, ryanodine receptor; SR, sarcoplasmic reticulum; TM, transmembrane.

RyR and IP_3R share ~ 17% sequence identity overall; however, the identity increases to ~ 35% within the predicted transmembrane region of the two proteins. It was also revealed that IP_3Rs are about half the size of RyRs. Despite the difference in molecular weight, the two receptors show similarities in their function and regulation. Both permeate Ca^{2+} and are regulated by it in a bell-shaped manner [11,12]; both are transmembrane (TM) proteins that share a high sequence homology in their ion-conducting pore; and both have conserved domains outside the TM region. These include the internal RyR and IP_3R homology [13] and mannosyl-transferase, IP_3R, RyR domains [14].

The present review focuses on recent advances in the structure–function studies on RyRs, highlighting new insights on the N-terminal domain (NTD), regulatory region and associating proteins of RyR. We also discuss the structural similarities between RyRs and IP_3Rs in light of structural data and genomic analyses of the two subfamilies of Ca^{2+} release channels.

Genomic analyses of the RyR and IP_3R NTD from unicellular to multicellular eukaryotes

In mammals, three different isoforms of RyRs exist. The first to be studied and cloned was RyR1 [15,16]. It is primarily expressed in skeletal muscle. RyR2 is highly expressed in cardiac muscle [17,18] but is also found in smooth muscle and the nervous system [19,20]. RyR3 is expressed at low levels in a variety of cell types including the nervous system and skeletal muscles of the diaphragm [20]. All three isoforms share ~ 66% sequence identity, the largest variation occurring in three 'divergent regions' encompassing residues 4254–4631 (D1), 1342–1403 (D2) and 1872–1923 (D3) in RyR1. Non-mammalian vertebrates such as chickens and bullfrogs express two RyR isoforms, RyRα and RyRβ [21,22], while lower organisms only express a single isoform [23,24]. Three isoforms of IP_3Rs (IP_3R1, IP_3R2 and IP_3R3) are also present in mammals [25–27]. They are ubiquitously expressed and have distinct cellular distribution patterns. In the nervous system IP_3R1 is predominantly expressed, whereas most other cell types express multiple isoforms [28–31]. Knockout studies for both RyR and IP_3R demonstrate their critical role in development and physiology. Mice missing *RyR1* die perinatally due to respiratory failure [32], *RyR2*-knockout mice die early during embryonic development [33], while mice missing *RyR3* are viable [34–36] but exhibit impaired social behavior [37–39]. *IP_3R*-knockout studies reveal that *IP_3R1*-deficient mice die *in utero* or by the weaning period [40], whereas *IP_3R2*- or *IP_3R3*-deficient mice exhibit physiological abnormalities such as decreased olfactory mucus secretion and hypoglycemia [41,42]. Additionally, many studies have linked mutations on the *RyR* genes to several human diseases (see Disease mutations), yet only one mutation in *IP_3R* has been associated with human disease [43].

Both *RyR* and *IP_3R* functional genes have been identified in a variety of multicellular eukaryotes ranging from *Caenorhabditis elegans* to human [44,45]. Recently, putative RyRs and IP_3Rs have also been observed in unicellular organisms such as *Salpingoeca rosetta*, *Monosiga brevicollis* and *Capsaspora owczarzaki* [46,47] as well as in pathogenic unicellular parasites including *Tryponosoma brucei*, *Tryponosoma cruzi*, *Leishmania infantum* and *Leishmania major* [13]. A recent study that examined the co-evolution of these two channels suggests that RyRs arose from ancestral IP_3R-like channels by incorporating promiscuous 'RyR' and 'SPRY' domains via horizontal gene transfer [48]. These genomic analyses suggest that RyRs and IP_3Rs have co-evolved from a common ancestor in unicellular species.

Despite the large difference in size, the two receptors share a similar architecture consisting of an NTD followed by a central regulatory domain that has various binding partners in both proteins yet is nearly twice as large in RyRs, a TM domain that contains the Ca^{2+}-conducting pore and a C-terminal tail (Fig. 1A). The recent structural determinations of the NTD for both proteins reveal conserved structural features [49–51]. It is with this structural conservation in mind that we examined the evolution of this region from unicellular to multicellular eukaryotes. The phylogenetic relationship of RyRs and IP_3Rs in unicellular and multicellular eukaryotes suggests that the NTD of IP_3R evolved from a lower organism RyR (Fig. 1B). This indicates that the inositol 1,4,5-trisphosphate (IP_3) binding ability of IP_3Rs was not always inherent and may have been attained during evolution. In fact, Arg and Lys residues involved in IP_3 coordination are less conserved in the lower eukaryotes, suggesting a mechanism whereby IP_3Rs evolutionarily acquired dual control by Ca^{2+} and IP_3.

Disease mutations

Several inheritable human diseases are associated with RyR mutations. Currently, none are associated with RyR3 mutations, but recent studies of neurodegenerative disorders such as Alzheimer's disease (AD) suggest that overexpression of RyR3 as well as altered expression of alternatively spliced variants of RyR2 and

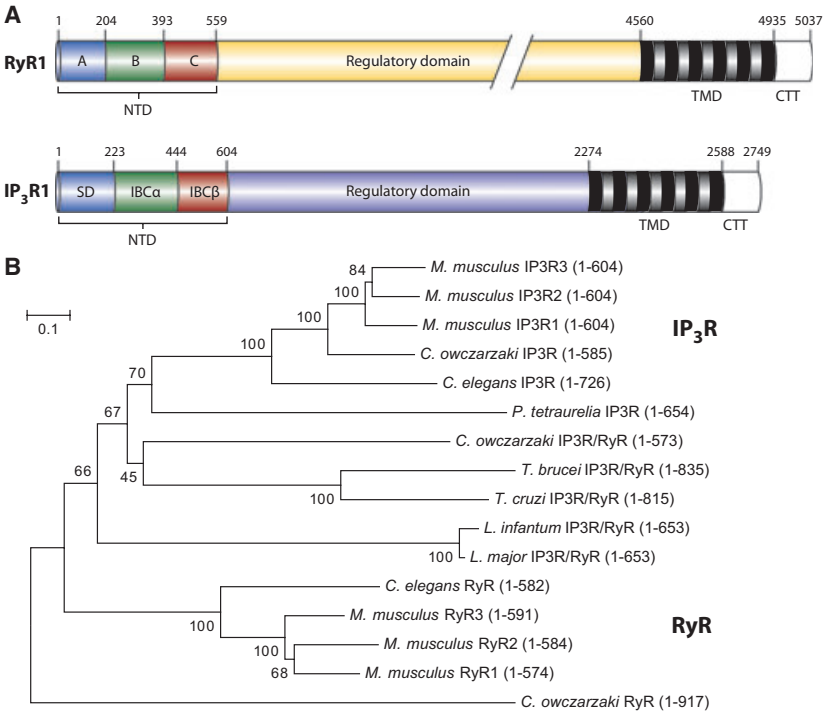

Fig. 1. Domain organization and genomic analyses of RyRs and IP_3Rs. (A) Domain architecture of RyR and IP_3R. Numbering used is from rabbit RyR1 and rat IP_3R1. NTD, N-terminal domain; SD, suppressor domain; IBC, IP_3 binding core; TMD, transmembrane domain; CTT, C-terminal tail. (B) A neighbor-joining phylogenetic tree showing the relationships of uni- and multi-cellular eukaryote homologues of IP_3Rs and RyRs. The numbers in parentheses represent the amino acid residues of the RyR and IP_3R homologues. Bootstrap values > 40 are shown at the nodes. The scale bar represents amino acid substitutions per site. Multiple sequence alignments were made with MUSCLE [144] using the default parameters. Neighbor-joining analysis was carried out using MEGA 5 [145].

RyR3 may play a role in the remodeling of neuronal Ca^{2+} signaling which leads to AD [52,53].

Mutations in RyR1 have been linked with malignant hyperthermia (MH) [54–57], central core disease (CCD) [58–60] and multiminicore disease [61]. MH is a pharmacogenetic disorder characterized by a rapid rise in body temperature, muscle rigidity and rhabdomyolysis in severe cases. An MH episode is usually triggered by a volatile anesthetic or a muscle relaxant, but in some cases stress can also be a trigger [62]. Administering dantrolene, a hydantoin derivative, effectively treats MH episodes. Since the first clinical use of dantrolene in the late 1970s [63], the mortality rate for MH episodes has decreased from ~ 80% to 5% today [64]. Although dantrolene inhibits RyR1 and studies have shown a direct interaction with RyR1 [65,66], its molecular mode of action remains unresolved. CCD is a congenital myopathy that usually presents during infancy and can lead to death. It is characterized by regions devoid of mitochondria in muscle fibers that histologically appear as circular 'cores' after oxidative staining [67,68]. Patients usually present with delayed motor development and hypotonia. Currently there are no known treatments for CCD.

Mutations associated with RyR2 can give rise to diseases associated with cardiac arrhythmias. Catecholaminergic polymorphic ventricular tachycardia (CPVT) gives rise to bidirectional ventricular tachycardia that can result in sudden death [69]. These episodes are usually triggered by physical or emotional stress and patients do not present any structural evidence of myocardial disease [70]. Another cardiac disease associated with RyR2 mutations is arrhythmogenic right ventricular dysplasia (ARVD). It is characterized by replacement of cardiac tissue with 'fibrofatty' deposits [71].

Well over 300 RyR mutations have been identified with a link to human disease. Most of these tend to cluster in three distinct regions on the protein: the N-terminal region (1–600), central region (~ 2100–2500) and the C-terminal region (~ 3900–5000) (Fig. 1A). It should be noted, however, that mutations have been found outside these regions (see Phosphorylation domain). Mutations associated with a specific disease tend to cluster in particular regions within RyRs. For instance, most MH mutations are found in the N-terminal and central region, while those of CCD are clustered in the C-terminal region [72]. Most mutation studies point to a gain-of-function hypothesis, whereby RyRs are rendered hypersensitive to activation either from the cytosolic [73] or luminal side of the receptor [74]. One model for this increased sensitivity or 'leakiness' is the 'zipper' model proposed by Ikemoto and colleagues [75,76]. In this model they suggest that the N-terminal and central regions interact

with each other. This interaction is thought to stabilize the channel in its closed state. Mutations clustered at interfaces between the N-terminal and central regions of RyR would weaken these normal interactions involved in the allostery of the channel, thereby destabilizing the closed state and rendering the channel more sensitive to stimuli. A caveat to this model is that it is based on the study of smaller peptides [77] as opposed to the larger folded N-terminal and central domains. Another and somewhat controversial model suggests that disruption of protein–protein interactions between RyR2 and the 12.6 kDa FK506 binding protein (FKBP12.6) alters the sensitivity of the channel to stimuli [78]. Dissociation of FKBP12.6 due to protein kinase A phosphorylation of RyR2 leads to increased sensitivity of the channel to cytosolic stimuli. Moreover, RyR2 mutations are also thought to weaken the FKBP12.6–RyR2 complex and hence lead to a leaky channel [79,80]. This FKBP12.6–RyR2 model has proved contentious as several groups have not been able to reproduce the results [81–85].

Regulators of RyR

Since ~ 80% of the RyR is found facing the cytosol, a wide array of proteins, small molecules and post-translational modifications are able to regulate the function of RyR in either a stimulatory or inhibitory fashion. Here, we highlight those that have been studied using high resolution structural methods. For a comprehensive review of RyR regulation see Lanner *et al*. [44].

Dihydropyridine receptor (DHPR)

DHPR is the voltage sensor in myocytes. It is composed of five subunits but only two are essential for E-C coupling in skeletal cells: the II–III loop of the α_{1S} subunit and the C-terminal tail of the β_{1a} subunit [86]. The II–III loop is well characterized as the critical interaction site for E-C coupling [87–91]. Depolarization is sensed by charged residues, which cause a conformational change in the loop that is physically transmitted to RyR1 [92]. One role of the β_{1a} subunit is to traffic the α_{1S} subunit to the t-tubule membrane; further, new studies show that it might also contribute directly to E-C coupling via its C-terminal tail [86,93]. Although DHPR is a key component of E-C coupling, two distinct mechanisms exist for triggering RyR opening and subsequent Ca^{2+} release from the SR into the cytosol. In cardiomyocytes, depolarization of the plasma membrane results in the opening of the DHPRs, which allows extracellular Ca^{2+} into the cytosol. This influx is sensed by RyR2, which binds Ca^{2+} and enables opening of the channel and a further influx of Ca^{2+} from the SR into the cytosol. This process is known as Ca^{2+}-induced Ca^{2+} release [94,95]. In skeletal muscles RyRs are intimately tied to DHPRs allowing a direct link between the two receptors [88,96]. In this scenario, two components of the DHPR interact with RyR1 in response to depolarization of the surface membrane. The sensitivity of DHPR to voltage changes at the plasma membrane results in a conformational change that is sensed by RyR1. Therefore, depolarization of the plasma membrane alone is sufficient to open RyR1. However, not all RyR1s are in direct contact with DHPR, and therefore those channels are activated by Ca^{2+} released from adjacent RyR1s through Ca^{2+}-induced Ca^{2+} release.

EF-hand containing proteins

Calmodulin (CaM) is a small (17 kDa) EF-hand containing Ca^{2+} binding protein that is able to fine-tune the activity of RyRs. It binds to the receptor in both its Ca^{2+}-bound (Ca^{2+}-CaM) and Ca^{2+}-free (apo-CaM) states [97,98]. Two overlapping yet distinct binding sites are proposed for apo- and Ca^{2+}-CaM on the tetrameric receptor [99], which is in close proximity to residues 3614–3643 in RyR1 and 3581–3612 in RyR2 [9,100]. Each RyR isoform is affected differently by CaM. Apo-CaM weakly activates RyR1, while Ca^{2+}-CaM inhibits RyR1 [97,98,100–102]. For RyR2, both apo-CaM and Ca^{2+}-CaM inhibit its activity [103,104]. The opposite effects of apo- and Ca^{2+}-CaM on RyR1 activity may be due to the structural consequences of Ca^{2+} binding to CaM. The structural fold of apo-CaM allows it to bind to the 'activating' binding site while Ca^{2+} binding to CaM results in its structural rearrangement allowing it to bind to the 'inhibitory' site. S100A1 is another EF-hand containing protein that binds and regulates RyRs. It enhances the activity of both RyR1 and RyR2 [105,106]. A crystal structure of Ca^{2+}-CaM bound to a RyR1 peptide (3614–3643) [107] and an NMR structure of S100A1 bound to two RyR1 peptides (3616–3627) [108] reveal that both proteins compete for the identical binding site by interacting with the same hydrophobic residues. A simplified model for apo-CaM, Ca^{2+}-CaM and S100A1 regulation proposes that under resting conditions S100A1 primarily regulates RyR1, allowing it to potentiate maximal Ca^{2+} release from the SR when it is stimulated. As Ca^{2+} becomes elevated in the cytosol, Ca^{2+}-CaM begins to compete out S100A1, thereby promoting channel inactivation [109].

High resolution structural studies of RyRs and its binding partners

Distal N-terminal domain (domain A)

The first reports highlighting atomic resolution structural features of folded RyR domains focused on the distal N-terminal domain (domain A) of RyR1 [110,111] and RyR2 [111,112] and their disease-associated mutants (Fig. 2A). These reports revealed that domain A folds into a β-trefoil made up of 12 β-strands and a single α-helix, which is similar to the structure of the suppressor domain of IP_3R [111]. Several disease-associated mutations corresponding to MH and CCD (RyR1A) and CPVT and ARVD (RyR2A) were mapped onto the two structures. Although there was some separation in the location of the mutants, most were localized to a loop connecting β8 to β9, termed the hot-spot (HS) loop. X-ray crystallography structures of RyR2A mutants, NMR studies of RyR1A mutants and biophysical analyses on both sets of mutants revealed minimal structural perturbations as well as no significant changes in structural stability, suggesting that these mutations may disrupt quaternary homotypic RyR interactions or heterotypic interactions with other regulatory partners [110,111].

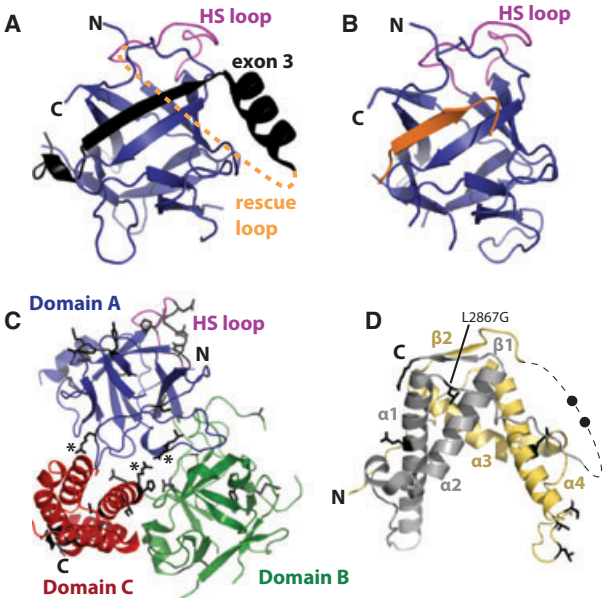

Fig. 2. High resolution crystal structures of folded domains in RyR. (A) Crystal structure of RyR2 domain A (PDB accession code 3IM5); secondary structure elements in black indicate residues encoded by exon 3. The rescue loop is represented as a dashed orange line and the HS loop is colored magenta. (B) Crystal structure of RyR2 Δ exon 3 mutant (PDB accession code 3QR5); rescue loop residues are colored as in (A). (C) Structure of RyR1ABC domain (PDB accession code 2XOA). Disease-associated mutations are shown in black. Mutations located at salt bridges are marked with asterisks. The HS loop is colored as in (A) and (B). (D) Crystal structure of RyR1 phosphorylation domain (PDB accession code 4ERT). Tandemly repeated RyR domains are shown in different colors (RyR domain 1 in gray and RyR domain 2 in gold). Side chains of disease-associated mutations are colored in black, and those not observed in the crystal structure are shown as black filled circles. The unstable mutant L2867G is highlighted.

RyR2A Δ exon 3

Recently, Lobo *et al.* investigated a mutant associated with a severe form of CPVT that employs a remarkable structural adaptation [112]. The mutant consists of a deletion encompassing the entire third exon of *RyR2* that encodes a 35-residue stretch made up of a β-strand and α-helix in RyR2A (Fig. 2A). Rather than this invasive deletion mutant inducing a misfolding, the structural fold of RyR2A is rescued by an insertion into the β-trefoil domain by a flexible loop immediately downstream from the deletion (Fig. 2A,B). This RyR2A Δ exon 3 mutant shows a significant increase in thermal stability which is incongruent with the severe nature of the disease state [111]. Therefore, it seems likely that the mutation disrupts intermolecular and/or intramolecular interactions that gate channel function, while enhancing the structural stability of the individual domain. Superimposing RyR2A Δ exon 3 with RyR1ABC allowed for docking of this domain onto the cryo-EM map [112]. The docking revealed that the α-helix from RyR2A is at an interface with electron dense columns that point toward the TM domain. Presumably, deletion of this helix in RyR2A Δ exon 3 would disrupt this interface and lead to aberrant channel activity.

RyR1ABC

The most comprehensive study of the NTD outlines the structural organization of the entire NTD (RyR1ABC) as well the location of 56 disease-associated mutations on its three-dimensional architecture [49] (Fig. 2C). RyR1ABC is composed of three domains, A–C. Domains A and B fold into β-trefoil cores and domain C is made of a five-helix bundle. All three domains are stabilized by hydrophilic interactions. The mapping of disease-associated mutations revealed that most are located at intramolecular interfaces between the three domains or at interfaces between ABC subunits in the tetrameric channel modeled by docking the high resolution ABC structures into the cryo-EM map [49] (see Cryo-electron microscopy). Close to a third of mutants (19 out of 56) map to an interface between domain A of

one ABC subunit and domain B of the adjacent subunit. This interface is made up of the HS loop found in domain A and two flexible loops in domain B. Another interface concentrated with mutations is located between domains A and C from the same subunit. Two salt bridges (Arg45 domain A and Asp447 domain C, and Asp61 and Glu40 domain A and Arg402 domain C) stabilize this interface [72]. Biophysical studies examining the effect of the Arg402Gly disease-associated mutation revealed minimal disruption in the fold and stability of RyR1ABC [49].

Phosphorylation domain

Recently, two groups independently solved the first crystal structures outside the NTD [113,114] (Fig. 2D). The phosphorylation domains from rabbit RyR1 (2734–2940) [113,114], mouse RyR2 (2699–2904) [114], human RyR3 (2597–2800) [114] and several disease-associated mutants [114] were solved to resolutions ranging from 1.6 to 2.2 Å. In both RyR1 and RyR2, the domain consists of a two-fold symmetrical structure in which each motif consists of two α-helices, one or more 3_{10} helix and a β-strand. A long and flexible loop separates each motif and contains the previously determined phosphorylation targets of S2843 (RyR1) and S2808/2814 (RyR2). A structure for a protein of unknown function from *Bacteroides thetaiotamicron* VPI-5482 (PDB accession code 3NRT) forms a homodimer that is strikingly similar to the phosphorylation domain of RyR [113,114]. Interestingly, a single copy of this 'RyR domain' encodes this unknown protein, and despite a low sequence similarity (~ 33%) the folding of these domains remains highly conserved.

There are 11 disease-associated mutations that can be mapped onto the phosphorylation domain structures. These can be divided into three groups: the first group contains seven mutants all found on the same face of the structure near the S2843 phosphorylation site; the second contains three mutants that are on the opposite face; while the last group contains the L2867G mutant (Fig. 2D). Most mutants have a minimal effect on the stability of the domain except for L2867G which demonstrated a melting temperature 13 °C lower than the wild type and readily aggregated and precipitated at room temperature [114]. This mutant did not crystallize, probably due to structural rearrangements caused by the disruption of hydrophobic interactions with other residues (i.e. L2871 and l2927) [114]. The E2764K crystal structure revealed minimal perturbations to the structure; however, a change in the surface charge was noted [113,114]. S2776M disrupts the hydrogen bond network that maintains the structure of a loop connecting α1 and α2, while R2939S disrupts three interactions: a salt bridge between E2870 and Q2877, hydrogen bonds with an ordered water molecule and van der Waals contact between the R2939 side chain and two buried residues (M2874 and W2821); yet for both mutants their structural integrity remains intact.

A previous study had shown that the most probable binding site for CaMKII was near R2840 since a mutation to Ala caused a 300-fold decrease in V_{max}/K_m for CaMKII [115]. Sharma *et al.* show that *in vivo* CaMKIIβ does indeed bind to the phosphorylation domain and that S2843A reduced this binding affinity by ~ 20% [113]. A possible reason for the modest decrease in binding affinity may be due to the fact that up to four additional phosphorylation sites in this area exist for CaMKII [114].

RyR1–DHPR interactions

Downstream from the NTD is a region encoding three 'SPRY' domains, so named because they were identified in both *Dictyostelium discoideum* tyrosine kinase spore lysis A (SplA) and the mammalian RyR [116]. SPRY domains normally function as protein–protein interaction motifs and are composed of a β-sandwich [117]. Although the precise function of SPRY domains in RyRs is still unknown, several reports support the idea that SPRY2 (residues S1085–V1208 in RyR1) plays a role in E-C coupling and, in fact, may be the binding partner for DHPR [118–120].

NMR studies carried out on the II–III loop of the α_{1S} subunit [120,121] and the C-terminal tail (V490–M524) of the β_{1a} subunit of DHPR [93] have probed the interaction with SPRY2 and *in vitro* work has demonstrated that the II–III loop of the α_{1S} subunit is an activator of RyR1 [122–124]. An NMR study revealed that the II–III loop of DHPR is intrinsically unstructured [120]. However, there was a propensity for two regions (A, residues 672–686, and B, 700–709) to form weak α-helices. The interaction between the II–III loop and SPRY2 was probed by monitoring the chemical shift perturbations (CSPs) in the II–III loop ^{1}H-^{15}N-HSQC spectra as a function of unlabeled SPRY2 concentration. The CSPs were clustered in the A and B region of the II–III loop. In addition, spin–spin relaxation (R2) rates were measured for the II–III loop alone or in complex with SPRY2 to probe for subtle conformational changes. The differences in R2 values were consistent with the measured affinity (equilibrium dissociation constant K_d ~ μM) for the II–III loop to SPRY2 [120]. These differences were most pronounced in the A region which corroborated the CSP data.

Binding studies probing the effect of mutating key residues in the A region of the II–III loop (681-RKRRK-685) revealed an eight-fold increase in K_d for SPRY2 indicating that this helical region of the II–III loop is critical for binding SPRY2 [120]. In order to stabilize the loop structure, similar to its native environment where it is bound to DHPR TM domains at the N- and C-termini, a follow-up study used intein-mediated technology to cyclize the loop [121]. This study showed that the cyclic loop stabilized the α-helices in the A and B region as evidenced by an increased secondary structure propensity score and elevated R2 values compared with the linear loop. The increased helical stability led to a three-fold increase in activation of RyR1 channels in SR vesicles [121].

A direct interaction between RyR1 and the C-terminal tail of the β_{1a} subunit of DHPR has also been demonstrated *in vitro* [125]. The C-terminal 35 residues form an α-helix that contains a hydrophobic surface containing three key residues (L496, L500 and W503) that bind to RyR1 [93]. By mutating all three residues to Ala, binding was abolished while the structural integrity of the helix was maintained. Including a hydrophobic heptad repeat, previously implicated in E-C coupling [126], to the N-terminus of the 35-residue tail did not increase RyR1 activation. Moreover, this study demonstrated that mutating this heptad repeat to Ala did not alter RyR1 activity [93]. Taken together, this new report suggests a key role for the hydrophobic face of the new helix from the C-terminal tail of the β_{1a} subunit. In contrast to this *in vitro* work, it has not been shown that β_{1a} can bind to RyR1 *in vivo* [127,128]. Therefore, future work is needed to establish the binding mechanism of β_{1a} to RyR1 as well the importance of the three key hydrophobic residues *in vivo*.

Cryo-electron microscopy

The large size of RyRs, their inherent dynamics and TM region make high resolution structural studies of the entire receptor extremely challenging. Advances in single-particle cryo electron microscopy (cryo-EM) have accelerated our understanding of the structure–function relationship in RyRs. Initial cryo-EM studies of RyR1 isolated from rabbit skeletal muscle examined the channel in the closed state at a resolution of ~ 2.4 nm [129,130]. Subsequent studies have pushed the resolution to ~ 10 Å [131,132]. These later studies reveal a tetrameric structure that is made up of a large cytoplasmic domain (~ 80% volume), with the remainder of the structure encompassing the TM region (Fig. 3A,C). The structure exhibits a four-fold

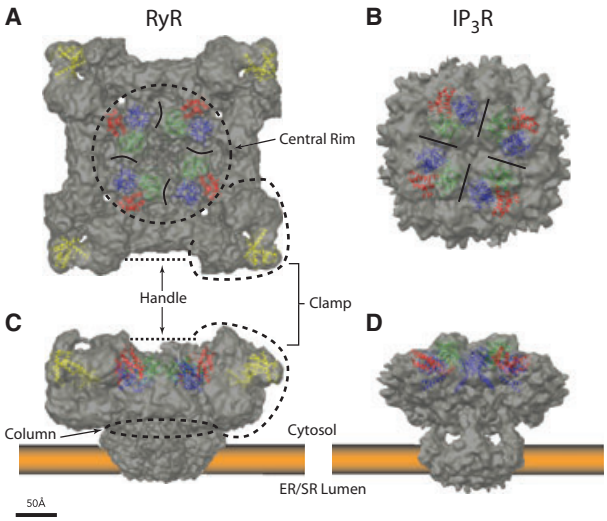

Fig. 3. Structural comparison of docked NTDs. Cryo-EM structures of RyR1 (A,C) (EMDB code 1275) and IP_3R1 (B,D) (EMDB code 5278) in the closed state are shown in top (A,B) and side view (C,D). Docked crystal structures of NTDs from RyR1 (PDB accession code 2XOA) and IP_3R (PDB accession code 3UJ0) are colored as in Fig. 1. Docked crystal structure of the phosphorylation domain (PDB accession code 4ERT) is colored in yellow. Dotted black lines indicate subregions with associated labels on the cryo-EM map of RyR1. Solid black line represents interfaces between different subunits. The scale bar applies to all panels in both dimensions. Docking was carried out as outlined in [49,50,114].

symmetry axis along the pore of the channel. The cytoplasmic region measures 270 × 270 × 100 Å, while the smaller TM region measures 120 × 120 × 60 Å. The former is full of cavities that separate distinct regions from one another and ostensibly provide access to a host of RyR regulators for docking onto the structure [72]. Several cytoplasmic subregions have been identified and are thought to play a role in the allosteric modulation of RyR. These include the 'clamp' and 'handle' regions as well as the 'central rim' [132,133] (Fig. 3A,C). A study characterizing the open and closed state of RyR1 at 10.2 Å revealed not only a change in channel pore size but also considerable changes in the conformation of the cytoplasmic region [134]. Specifically, the clamp region moved down towards the SR membrane by ~ 8 Å, while the central rim moved up towards the t-tubules by 4 Å. In addition there is evidence for a twisting motion in the TM region [134]. These studies reveal that RyR undergoes allosteric coupling between the distinct regions in its transition from open to closed state, with easy access for its regulators to modulate this coupling.

The insertion of green fluorescent fusion proteins (GFPs) or antibody epitopes into full-length RyRs has

facilitated approximations of the location of several RyR regions and accessory proteins in the tetrameric receptor (reviewed by Kimlicka and Van Petegem [135]). A caveat of these studies, however, is that the chromophoric center of fluorescent proteins inserted into RyR which report on relative localization can be as far away as 45 Å from the insertion site inferred from primary sequence [136].

The increased resolution of recent cryo-EM maps for RyR1 in the open and closed state along with fluorescence resonance energy transfer and antibody-based cryo-EM studies have provided insight into quaternary interactions during channel opening and approximate locations of RyR regulatory partners. Additionally, it has advanced our knowledge of the architectural arrangement of individual domains in RyR.

Docking of RyR1ABC into the cryo-EM map of RyR1 revealed that the NTD forms a vestibule around the four-fold symmetry axis [49]. A number of disease-associated mutations within RyR1ABC are located in the interfaces between different subunits (Fig. 3A). By comparing the cryo-EM maps of the open and closed states, subtle changes in the cytoplasmic domain can be seen, which indicate global conformational changes that are thought to affect interfaces between individual subunits [134]. It is probable that mutations located at these interfaces weaken the interactions, facilitating the opening of the channel.

The independent docking by two groups of the phosphorylation domain into the cryo-EM map of RyR1 placed it in the clamp region [113,114] (Fig. 3A, C). The results are compatible with previous cryo-EM studies that used GFPs to generate difference maps showing the approximate location of this phosphorylation domain [137]. The fact that there is ambiguity in the exact orientation may be due to the increased flexibility of this region as it has been shown to move ~ 8 Å toward the SR membrane during channel opening [134]. Interestingly, the location also coincides with a region implicated in mediating contacts with neighboring RyRs [138,139].

Structural comparison between RyRs and IP_3Rs

The recent determination of high resolution crystal structures for the NTDs of RyR (RyR1ABC) [49] and IP_3R (IP_3R-NT) [50,51] along with improved cryo-EM maps of the full-length RyR [131,132] and IP_3R [140] has revealed organizational similarities at the domain level and in the context of functional tetramers. Individual domains from RyR1ABC and IP_3R-NT superimpose very well despite only 19–25% sequence identity [141]. Moreover, their relative orientation is similar with an rmsd of < 3 Å. In fact, the critical gating loop in IP_3R and the HS loop in RyR show remarkable structural conservation [50] indicative of the importance of this structural feature to the mechanistic action of both receptors. Both NTDs form tetrameric rings around a four-fold symmetry axis with similar positions for each domain (Fig. 3A,B). This similarity in structure extends to their function as demonstrated by chimeric studies [50]. Deleting the suppressor domain of IP_3R results in defective gating [142]. Seo *et al.* [50] demonstrated that exchanging domain A of RyR1 with the suppressor domain of IP_3R recapitulates IP_3-dependent channel opening and reproduces the effect of the suppressor domain. These results demonstrate that the two domains can be functionally swapped, consistent with the notion of a common ancestry indicated by our phylogenetic analysis (Fig. 1). This chimera study was also extended to the TM region of IP_3R, where the C-terminal TM region was swapped with the corresponding RyR region [50]. Again IP_3 was able to activate this chimera, demonstrating a common gating mechanism between the two receptors. Taken together, these data strongly support the co-evolution of these two receptors, allowing key domains to be swapped with retention of function.

Conclusions

The last decade has provided the first high resolution structures of these critically important Ca^{2+} release channels. It is evident from these and cryo-EM studies that the N-terminus of both receptors plays a crucial role in gating the two channels. EM studies show that the central rim of RyR experiences large movements during channel opening and closing. It is possible that disease-associated mutations disrupt these allosteric movements, thereby perturbing the normal function of the channel (Fig. 4A,C). The large distance between the two investigated cytosolic regions (NTD and phosphorylation domain) and the TM domain precludes any direct interaction. It remains to be determined which parts of the regulatory region are the crucial link that relays information to the pore. This scenario is also mirrored in IP_3R where the same domain architecture is present (Fig. 4B,D). Again, the large distances between the pore and IP_3R-NT suggest the involvement of other parts of the receptors, despite an earlier biochemical study which proposed a hypothetical model of direct coupling between the pore and the IP_3R-NT [143].

Our evolutionary analysis suggests that IP_3R-NT evolved from a lower order RyR (Fig. 1). The

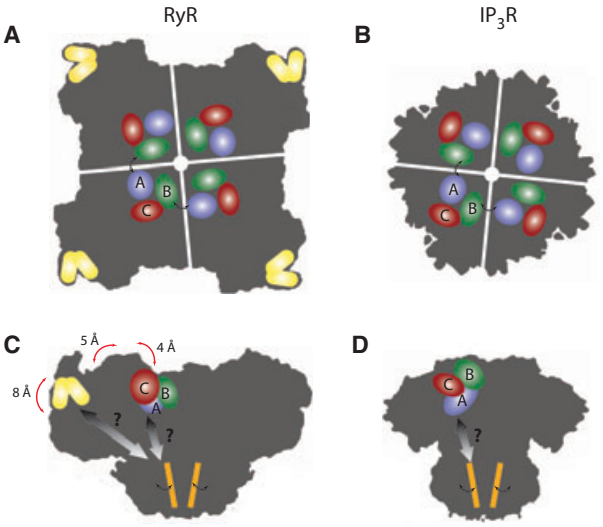

Fig. 4. Model of coupling between the TM domain and NTD via the regulatory domain in RyR and IP_3R. Cartoon representation of the proposed gating mechanism for both receptors. Panels and coloring are the same as in Fig. 3. (A), (B) Double headed arrows represent proposed allosteric interactions between domains on different subunits. (C) Red double headed arrows represent observed movement caused by the opening of RyR1. Estimated distances are indicated in angstroms (Å). (D) Small black double headed arrows represent proposed movement by TM segments during channel opening. Gradient arrows in (C) and (D) indicate hypothetical allosteric interactions between the TM domain and NTD in RyR1 and IP_3R. These interactions most probably occur via the regulatory domain which may interact with the A/suppressor domain from RyR1 and IP_3R.

remarkable structural similarities observed between RyR1ABC and IP_3R-NT and the functional interchangeability of these domains strongly support this notion. It is noteworthy that the primary sequences of RyRs are almost twice as large as the IP_3Rs, implying that RyRs may have a larger array of small molecule and protein regulators than IP_3Rs. Further work is needed to test this notion, as important questions still remain unanswered: where are the Ca^{2+} binding sites for both proteins and how does this divalent cation regulate receptor activity; what are the structural mechanisms for RyR regulation by key partners such as DHPR, FKBP and ATP, to name a few; how do these binding partners affect the observed allosteric interactions in the tetrameric context of RyR? Understanding the structural mechanisms of receptor function for these vital Ca^{2+} release channels will promote new rationale and approaches to the treatment of myriad Ca^{2+}-signaled malignancies and increase our understanding of fundamental physiological mechanisms in human health.

Acknowledgements

We are grateful for discussions with David MacLennan, Colin Taylor, Filip Van Petegem and Katsuhiko Mikoshiba. This work was supported by HSFC, CIHR and NSERC. FJA holds a Frederick Banting and Charles Best Graduate Scholarship Doctoral Award. MI holds the Canada Research Chair in Cancer Structural Biology.

References

1 Lewartowski B (2000) Excitation–contraction coupling in cardiac muscle revisited. *J Physiol Pharmacol* **51**, 371–386.
2 Lamb GD (2000) Excitation–contraction coupling in skeletal muscle: comparisons with cardiac muscle. *Clin Exp Pharmacol Physiol* **27**, 216–224.
3 Beam KG & Bannister RA (2010) Looking for answers to EC coupling's persistent questions. *J Gen Physiol* **136**, 7–12.
4 Franzini-Armstrong C (1970) Studies of the Triad: I. Structure of the junction in Frog Twitch fibers. *J Cell Biol* **47**, 488–499.
5 Campbell KP, Knudson CM, Imagawa T, Leung AT, Sutko JL, Kahl SD, Raab CR & Madson L (1987) Identification and characterization of the high affinity [3H]ryanodine receptor of the junctional sarcoplasmic reticulum Ca2 + release channel. *J Biol Chem* **262**, 6460–6463.
6 Inui M, Saito A & Fleischer S (1987) Purification of the ryanodine receptor and identity with feet structures of junctional terminal cisternae of sarcoplasmic reticulum from fast skeletal muscle. *J Biol Chem* **262**, 1740–1747.
7 Lai FA, Erickson HP, Rousseau E, Liu QY & Meissner G (1988) Purification and reconstitution of the calcium release channel from skeletal muscle. *Nature* **331**, 315–319.
8 Rogers EF, Koniuszy FR, Shavel J Jr. & Folkers K (1948) Plant insecticides; ryanodine, a new alkaloid from *Ryania speciosa* Vahl. *J Am Chem Soc* **70**, 3086–3088.
9 Mignery GA, Sudhof TC, Takei K & De Camilli P (1989) Putative receptor for inositol 1,4,5-trisphosphate similar to ryanodine receptor. *Nature* **342**, 192–195.
10 Furuichi T, Yoshikawa S & Mikoshiba K (1989) Nucleotide sequence of cDNA encoding P400 protein in the mouse cerebellum. *Nucleic Acids Res* **17**, 5385–5386.
11 Tu H, Wang Z & Bezprozvanny I (2005) Modulation of mammalian inositol 1,4,5-trisphosphate receptor isoforms by calcium: a role of calcium sensor region. *Biophys J* **88**, 1056–1069.
12 Roderick HL, Berridge MJ & Bootman MD (2003) Calcium-induced calcium release. *Curr Biol* **13**, R425.

13 Prole DL & Taylor CW (2011) Identification of intracellular and plasma membrane calcium channel homologues in pathogenic parasites. *PLoS One* **6**, e26218.
14 Ponting CP (2000) Novel repeats in ryanodine and IP3 receptors and protein O-mannosyltransferases. *Trends Biochem Sci* **25**, 48–50.
15 Takeshima H, Nishimura S, Matsumoto T, Ishida H, Kangawa K, Minamino N, Matsuo H, Ueda M, Hanaoka M, Hirose T *et al.* (1989) Primary structure and expression from complementary DNA of skeletal muscle ryanodine receptor. *Nature* **339**, 439–445.
16 Zorzato F, Fujii J, Otsu K, Phillips M, Green NM, Lai FA, Meissner G & MacLennan DH (1990) Molecular cloning of cDNA encoding human and rabbit forms of the Ca2 + release channel (ryanodine receptor) of skeletal muscle sarcoplasmic reticulum. *J Biol Chem* **265**, 2244–2256.
17 Otsu K, Willard HF, Khanna VK, Zorzato F, Green NM & MacLennan DH (1990) Molecular cloning of cDNA encoding the Ca2 + release channel (ryanodine receptor) of rabbit cardiac muscle sarcoplasmic reticulum. *J Biol Chem* **265**, 13472–13483.
18 Nakai J, Imagawa T, Hakamat Y, Shigekawa M, Takeshima H & Numa S (1990) Primary structure and functional expression from cDNA of the cardiac ryanodine receptor/calcium release channel. *FEBS Lett* **271**, 169–177.
19 Coussin F, Macrez N, Morel JL & Mironneau J (2000) Requirement of ryanodine receptor subtypes 1 and 2 for Ca(2 +)-induced Ca(2 +) release in vascular myocytes. *J Biol Chem* **275**, 9596–9603.
20 Giannini G, Conti A, Mammarella S, Scrobogna M & Sorrentino V (1995) The ryanodine receptor/calcium channel genes are widely and differentially expressed in murine brain and peripheral tissues. *J Cell Biol* **128**, 893–904.
21 Ottini L, Marziali G, Conti A, Charlesworth A & Sorrentino V (1996) Alpha and beta isoforms of ryanodine receptor from chicken skeletal muscle are the homologues of mammalian RyR1 and RyR3. *Biochem J* **315**, 207–216.
22 Oyamada H, Murayama T, Takagi T, Iino M, Iwabe N, Miyata T, Ogawa Y & Endo M (1994) Primary structure and distribution of ryanodine-binding protein isoforms of the bullfrog skeletal muscle. *J Biol Chem* **269**, 17206–17214.
23 Maryon EB, Coronado R & Anderson P (1996) unc-68 encodes a ryanodine receptor involved in regulating *C. elegans* body-wall muscle contraction. *J Cell Biol* **134**, 885–893.
24 Takeshima H, Nishi M, Iwabe N, Miyata T, Hosoya T, Masai I & Hotta Y (1994) Isolation and characterization of a gene for a ryanodine receptor/calcium release channel in *Drosophila melanogaster*. *FEBS Lett* **337**, 81–87.
25 Iwai M, Tateishi Y, Hattori M, Mizutani A, Nakamura T, Futatsugi A, Inoue T, Furuichi T, Michikawa T & Mikoshiba K (2005) Molecular cloning of mouse type 2 and type 3 inositol 1,4,5-trisphosphate receptors and identification of a novel type 2 receptor splice variant. *J Biol Chem* **280**, 10305–10317.
26 De Smedt F, Verjans B, Mailleux P & Erneux C (1994) Cloning and expression of human brain type I inositol 1,4,5-trisphosphate 5-phosphatase. High levels of mRNA in cerebellar Purkinje cells. *FEBS Lett* **347**, 69–72.
27 Blondel O, Takeda J, Janssen H, Seino S & Bell GI (1993) Sequence and functional characterization of a third inositol trisphosphate receptor subtype, IP3R-3, expressed in pancreatic islets, kidney, gastrointestinal tract, and other tissues. *J Biol Chem* **268**, 11356–11363.
28 Bush KT, Stuart RO, Li SH, Moura LA, Sharp AH, Ross CA & Nigam SK (1994) Epithelial inositol 1,4,5-trisphosphate receptors. Multiplicity of localization, solubility, and isoforms. *J Biol Chem* **269**, 23694–23699.
29 De Smedt H, Missiaen L, Parys JB, Henning RH, Sienaert I, Vanlingen S, Gijsens A, Himpens B & Casteels R (1997) Isoform diversity of the inositol trisphosphate receptor in cell types of mouse origin. *Biochem J* **322**, 575–583.
30 Newton CL, Mignery GA & Sudhof TC (1994) Co-expression in vertebrate tissues and cell lines of multiple inositol 1,4,5-trisphosphate (InsP3) receptors with distinct affinities for InsP3. *J Biol Chem* **269**, 28613–28619.
31 Shibao K, Hirata K, Robert ME & Nathanson MH (2003) Loss of inositol 1,4,5-trisphosphate receptors from bile duct epithelia is a common event in cholestasis. *Gastroenterology* **125**, 1175–1187.
32 Takeshima H, Iino M, Takekura H, Nishi M, Kuno J, Minowa O, Takano H & Noda T (1994) Excitation–contraction uncoupling and muscular degeneration in mice lacking functional skeletal muscle ryanodine-receptor gene. *Nature* **369**, 556–559.
33 Takeshima H, Komazaki S, Hirose K, Nishi M, Noda T & Iino M (1998) Embryonic lethality and abnormal cardiac myocytes in mice lacking ryanodine receptor type 2. *EMBO J* **17**, 3309–3316.
34 Takeshima H, Ikemoto T, Nishi M, Nishiyama N, Shimuta M, Sugitani Y, Kuno J, Saito I, Saito H, Endo M *et al.* (1996) Generation and characterization of mutant mice lacking ryanodine receptor type 3. *J Biol Chem* **271**, 19649–19652.
35 Futatsugi A, Kato K, Ogura H, Li ST, Nagata E, Kuwajima G, Tanaka K, Itohara S & Mikoshiba K (1999) Facilitation of NMDAR-independent LTP and

spatial learning in mutant mice lacking ryanodine receptor type 3. *Neuron* **24**, 701–713.
36 Bertocchini F, Ovitt CE, Conti A, Barone V, Scholer HR, Bottinelli R, Reggiani C & Sorrentino V (1997) Requirement for the ryanodine receptor type 3 for efficient contraction in neonatal skeletal muscles. *EMBO J* **16**, 6956–6963.
37 Matsuo N, Tanda K, Nakanishi K, Yamasaki N, Toyama K, Takao K, Takeshima H & Miyakawa T (2009) Comprehensive behavioral phenotyping of ryanodine receptor type 3 (RyR3) knockout mice: decreased social contact duration in two social interaction tests. *Front Behav Neurosci* **3**, 3.
38 Kouzu Y, Moriya T, Takeshima H, Yoshioka T & Shibata S (2000) Mutant mice lacking ryanodine receptor type 3 exhibit deficits of contextual fear conditioning and activation of calcium/calmodulin-dependent protein kinase II in the hippocampus. *Brain Res Mol Brain Res* **76**, 142–150.
39 Balschun D, Wolfer DP, Bertocchini F, Barone V, Conti A, Zuschratter W, Missiaen L, Lipp HP, Frey JU & Sorrentino V (1999) Deletion of the ryanodine receptor type 3 (RyR3) impairs forms of synaptic plasticity and spatial learning. *EMBO J* **18**, 5264–5273.
40 Matsumoto M, Nakagawa T, Inoue T, Nagata E, Tanaka K, Takano H, Minowa O, Kuno J, Sakakibara S, Yamada M *et al.* (1996) Ataxia and epileptic seizures in mice lacking type 1 inositol 1,4,5-trisphosphate receptor. *Nature* **379**, 168–171.
41 Futatsugi A, Nakamura T, Yamada MK, Ebisui E, Nakamura K, Uchida K, Kitaguchi T, Takahashi-Iwanaga H, Noda T, Aruga J *et al.* (2005) IP3 receptor types 2 and 3 mediate exocrine secretion underlying energy metabolism. *Science* **309**, 2232–2234.
42 Fukuda N, Shirasu M, Sato K, Ebisui E, Touhara K & Mikoshiba K (2008) Decreased olfactory mucus secretion and nasal abnormality in mice lacking type 2 and type 3 IP3 receptors. *Eur J Neurosci* **27**, 2665–2675.
43 Yamazaki H, Nozaki H, Onodera O, Michikawa T, Nishizawa M & Mikoshiba K (2011) Functional characterization of the P1059L mutation in the inositol 1,4,5-trisphosphate receptor type 1 identified in a Japanese SCA15 family. *Biochem Biophys Res Commun* **410**, 754–758.
44 Lanner JT, Georgiou DK, Joshi AD & Hamilton SL (2010) Ryanodine receptors: structure, expression, molecular details, and function in calcium release. *Cold Spring Harb Perspect Biol* **2**, a003996.
45 Bezprozvanny I (2005) The inositol 1,4,5-trisphosphate receptors. *Cell Calcium* **38**, 261–272.
46 Cai X (2008) Unicellular Ca2 + signaling 'toolkit' at the origin of metazoa. *Mol Biol Evol* **25**, 1357–1361.
47 Cai X & Clapham DE (2012) Ancestral Ca2 + signaling machinery in early animal and fungal evolution. *Mol Biol Evol* **29**, 91–100.
48 Mackrill JJ (2012) Ryanodine receptor calcium release channels: an evolutionary perspective. *Adv Exp Med Biol* **740**, 159–182.
49 Tung C-C, Lobo PA, Kimlicka L & Van Petegem F (2010) The amino-terminal disease hotspot of ryanodine receptors forms a cytoplasmic vestibule. *Nature* **468**, 585–588.
50 Seo MD, Velamakanni S, Ishiyama N, Stathopulos PB, Rossi AM, Khan SA, Dale P, Li C, Ames JB, Ikura M *et al.* (2012) Structural and functional conservation of key domains in InsP3 and ryanodine receptors. *Nature* **483**, 108–112.
51 Lin CC, Baek K & Lu Z (2011) Apo and InsP(3)-bound crystal structures of the ligand-binding domain of an InsP(3) receptor. *Nat Struct Mol Biol* **18**, 1172–1174.
52 Bruno AM, Huang JY, Bennett DA, Marr RA, Hastings ML & Stutzmann GE (2012) Altered ryanodine receptor expression in mild cognitive impairment and Alzheimer's disease. *Neurobiol Aging* **33**, e1001–e1006.
53 Berridge MJ (2011) Calcium signalling and Alzheimer's disease. *Neurochem Res* **36**, 1149–1156.
54 Brandom BW, Larach MG, Chen MS & Young MC (2011) Complications associated with the administration of dantrolene 1987 to 2006: a report from the North American Malignant Hyperthermia Registry of the Malignant Hyperthermia Association of the United States. *Anesth Analg* **112**, 1115–1123.
55 Durham WJ, Aracena-Parks P, Long C, Rossi AE, Goonasekera SA, Boncompagni S, Galvan DL, Gilman CP, Baker MR, Shirokova N *et al.* (2008) RyR1 S-nitrosylation underlies environmental heat stroke and sudden death in Y522S RyR1 knockin mice. *Cell* **133**, 53–65.
56 Hwang JH, Zorzato F, Clarke NF & Treves S (2012) Mapping domains and mutations on the skeletal muscle ryanodine receptor channel. *Trends Mol Med* **18**, 644–657.
57 Jurkat-Rott K, McCarthy T & Lehmann-Horn F (2000) Genetics and pathogenesis of malignant hyperthermia. *Muscle Nerve* **23**, 4–17.
58 Avila G & Dirksen RT (2001) Functional effects of central core disease mutations in the cytoplasmic region of the skeletal muscle ryanodine receptor. *J Gen Physiol* **118**, 277–290.
59 Jungbluth H (2007) Central core disease. *Orphanet J Rare Dis* **2**, 25.
60 Robinson RL, Brooks C, Brown SL, Ellis FR, Halsall PJ, Quinnell RJ, Shaw MA & Hopkins PM (2002) RYR1 mutations causing central core disease are associated with more severe malignant hyperthermia *in vitro* contracture test phenotypes. *Hum Mutat* **20**, 88–97.
61 Jungbluth H (2007) Multi-minicore disease. *Orphanet J Rare Dis* **2**, 31.

62 Capacchione JF & Muldoon SM (2009) The relationship between exertional heat illness, exertional rhabdomyolysis, and malignant hyperthermia. *Anesth Analg* **109**, 1065–1069.
63 Kolb ME, Horne ML & Martz R (1982) Dantrolene in human malignant hyperthermia. *Anesthesiology* **56**, 254–262.
64 Rosero EB, Adesanya AO, Timaran CH & Joshi GP (2009) Trends and outcomes of malignant hyperthermia in the United States, 2000 to 2005. *Anesthesiology* **110**, 89–94.
65 Paul-Pletzer K, Yamamoto T, Bhat MB, Ma J, Ikemoto N, Jimenez LS, Morimoto H, Williams PG & Parness J (2002) Identification of a dantrolene-binding sequence on the skeletal muscle ryanodine receptor. *J Biol Chem* **277**, 34918–34923.
66 Zhao F, Li P, Chen SR, Louis CF & Fruen BR (2001) Dantrolene inhibition of ryanodine receptor Ca2 + release channels. Molecular mechanism and isoform selectivity. *J Biol Chem* **276**, 13810–13816.
67 MacLennan DH & Phillips MS (1992) Malignant hyperthermia. *Science* **256**, 789–794.
68 Sewry CA, Muller C, Davis M, Dwyer JS, Dove J, Evans G, Schroder R, Furst D, Helliwell T, Laing N *et al.* (2002) The spectrum of pathology in central core disease. *Neuromuscul Disord* **12**, 930–938.
69 Laitinen PJ, Brown KM, Piippo K, Swan H, Devaney JM, Brahmbhatt B, Donarum EA, Marino M, Tiso N, Viitasalo M *et al.* (2001) Mutations of the cardiac ryanodine receptor (RyR2) gene in familial polymorphic ventricular tachycardia. *Circulation* **103**, 485–490.
70 Lehnart SE, Wehrens XH, Laitinen PJ, Reiken SR, Deng SX, Cheng Z, Landry DW, Kontula K, Swan H & Marks AR (2004) Sudden death in familial polymorphic ventricular tachycardia associated with calcium release channel (ryanodine receptor) leak. *Circulation* **109**, 3208–3214.
71 El Masry HZ & Yadav AV (2008) Arrhythmogenic right ventricular dysplasia/cardiomyopathy. *Expert Rev Cardiovasc Ther* **6**, 249–260.
72 Van Petegem F (2012) Ryanodine receptors: structure and function. *J Biol Chem* **287**, 31624–31632.
73 Tong J, Oyamada H, Demaurex N, Grinstein S, McCarthy TV & MacLennan DH (1997) Caffeine and halothane sensitivity of intracellular Ca2 + release is altered by 15 calcium release channel (ryanodine receptor) mutations associated with malignant hyperthermia and/or central core disease. *J Biol Chem* **272**, 26332–26339.
74 Jiang D, Xiao B, Yang D, Wang R, Choi P, Zhang L, Cheng H & Chen SR (2004) RyR2 mutations linked to ventricular tachycardia and sudden death reduce the threshold for store-overload-induced Ca2 + release (SOICR). *Proc Natl Acad Sci USA* **101**, 13062–13067.
75 Tateishi H, Yano M, Mochizuki M, Suetomi T, Ono M, Xu X, Uchinoumi H, Okuda S, Oda T, Kobayashi S *et al.* (2009) Defective domain–domain interactions within the ryanodine receptor as a critical cause of diastolic Ca2 + leak in failing hearts. *Cardiovasc Res* **81**, 536–545.
76 Suetomi T, Yano M, Uchinoumi H, Fukuda M, Hino A, Ono M, Xu X, Tateishi H, Okuda S, Doi M *et al.* (2011) Mutation-linked defective interdomain interactions within ryanodine receptor cause aberrant Ca2 + release leading to catecholaminergic polymorphic ventricular tachycardia/clinical perspective. *Circulation* **124**, 682–694.
77 Ikemoto N & Yamamoto T (2000) Postulated role of inter-domain interaction within the ryanodine receptor in Ca(2 +) channel regulation. *Trends Cardiovasc Med* **10**, 310–316.
78 Marx SO, Reiken S, Hisamatsu Y, Jayaraman T, Burkhoff D, Rosemblit N & Marks AR (2000) PKA phosphorylation dissociates FKBP12.6 from the calcium release channel (ryanodine receptor): defective regulation in failing hearts. *Cell* **101**, 365–376.
79 Wehrens XH, Lehnart SE, Huang F, Vest JA, Reiken SR, Mohler PJ, Sun J, Guatimosim S, Song LS, Rosemblit N *et al.* (2003) FKBP12.6 deficiency and defective calcium release channel (ryanodine receptor) function linked to exercise-induced sudden cardiac death. *Cell* **113**, 829–840.
80 Lehnart SE, Mongillo M, Bellinger A, Lindegger N, Chen BX, Hsueh W, Reiken S, Wronska A, Drew LJ, Ward CW *et al.* (2008) Leaky Ca2 + release channel/ryanodine receptor 2 causes seizures and sudden cardiac death in mice. *J Clin Invest* **118**, 2230–2245.
81 George CH, Higgs GV & Lai FA (2003) Ryanodine receptor mutations associated with stress-induced ventricular tachycardia mediate increased calcium release in stimulated cardiomyocytes. *Circ Res* **93**, 531–540.
82 Guo T, Cornea RL, Huke S, Camors E, Yang Y, Picht E, Fruen BR & Bers DM (2010) Kinetics of FKBP12.6 binding to ryanodine receptors in permeabilized cardiac myocytes and effects on Ca sparks. *Circ Res* **106**, 1743–1752.
83 Jiang D, Wang R, Xiao B, Kong H, Hunt DJ, Choi P, Zhang L & Chen SR (2005) Enhanced store overload-induced Ca2 + release and channel sensitivity to luminal Ca2 + activation are common defects of RyR2 mutations linked to ventricular tachycardia and sudden death. *Circ Res* **97**, 1173–1181.
84 Liu N, Colombi B, Memmi M, Zissimopoulos S, Rizzi N, Negri S, Imbriani M, Napolitano C, Lai FA & Priori SG (2006) Arrhythmogenesis in catecholaminergic polymorphic ventricular tachycardia: insights from a RyR2 R4496C knock-in mouse model. *Circ Res* **99**, 292–298.

85 Xiao J, Tian X, Jones PP, Bolstad J, Kong H, Wang R, Zhang L, Duff HJ, Gillis AM, Fleischer S *et al.* (2007) Removal of FKBP12.6 does not alter the conductance and activation of the cardiac ryanodine receptor or the susceptibility to stress-induced ventricular arrhythmias. *J Biol Chem* **282**, 34828–34838.
86 Karunasekara Y, Dulhunty AF & Casarotto MG (2009) The voltage-gated calcium-channel beta subunit: more than just an accessory. *Eur Biophys J* **39**, 75–81.
87 Wilkens CM, Kasielke N, Flucher BE, Beam KG & Grabner M (2001) Excitation–contraction coupling is unaffected by drastic alteration of the sequence surrounding residues L720–L764 of the alpha 1S II–III loop. *Proc Natl Acad Sci USA* **98**, 5892–5897.
88 Tanabe T, Beam KG, Adams BA, Niidome T & Numa S (1990) Regions of the skeletal muscle dihydropyridine receptor critical for excitation–contraction coupling. *Nature* **346**, 567–569.
89 Kugler G, Weiss RG, Flucher BE & Grabner M (2004) Structural requirements of the dihydropyridine receptor alpha1S II–III loop for skeletal-type excitation–contraction coupling. *J Biol Chem* **279**, 4721–4728.
90 Kugler G, Grabner M, Platzer J, Striessnig J & Flucher BE (2004) The monoclonal antibody mAB 1A binds to the excitation–contraction coupling domain in the II–III loop of the skeletal muscle calcium channel alpha(1S) subunit. *Arch Biochem Biophys* **427**, 91–100.
91 Carbonneau L, Bhattacharya D, Sheridan DC & Coronado R (2005) Multiple loops of the dihydropyridine receptor pore subunit are required for full-scale excitation–contraction coupling in skeletal muscle. *Biophys J* **89**, 243–255.
92 Dulhunty AF, Haarmann CS, Green D, Laver DR, Board PG & Casarotto MG (2002) Interactions between dihydropyridine receptors and ryanodine receptors in striated muscle. *Prog Biophys Mol Biol* **79**, 45–75.
93 Karunasekara Y, Rebbeck RT, Weaver LM, Board PG, Dulhunty AF & Casarotto MG (2012) An alpha-helical C-terminal tail segment of the skeletal L-type Ca2 + channel beta1a subunit activates ryanodine receptor type 1 via a hydrophobic surface. *FASEB J.* **26**, 5049–5059.
94 Fabiato A (1983) Calcium-induced release of calcium from the cardiac sarcoplasmic reticulum. *Am J Physiol* **245**, C1–14.
95 Endo M, Tanaka M & Ogawa Y (1970) Calcium induced release of calcium from the sarcoplasmic reticulum of skinned skeletal muscle fibres. *Nature* **228**, 34–36.
96 Rios E & Brum G (1987) Involvement of dihydropyridine receptors in excitation–contraction coupling in skeletal muscle. *Nature* **325**, 717–720.
97 Damiani E & Margreth A (2000) Pharmacological clues to calmodulin-mediated activation of skeletal ryanodine receptor using [3H]-ryanodine binding. *J Muscle Res Cell Motil* **21**, 1–8.
98 Rodney GG, Williams BY, Strasburg GM, Beckingham K & Hamilton SL (2000) Regulation of RYR1 activity by Ca(2 +) and calmodulin. *Biochemistry* **39**, 7807–7812.
99 Huang X, Fruen B, Farrington DT, Wagenknecht T & Liu Z (2012) Calmodulin-binding locations on the skeletal and cardiac ryanodine receptors. *J Biol Chem* **287**, 30328–30335.
100 Yamaguchi N, Xin C & Meissner G (2001) Identification of apocalmodulin and Ca2 + -calmodulin regulatory domain in skeletal muscle Ca2 + release channel, ryanodine receptor. *J Biol Chem* **276**, 22579–22585.
101 Buratti R, Prestipino G, Menegazzi P, Treves S & Zorzato F (1995) Calcium dependent activation of skeletal muscle Ca2 + release channel (ryanodine receptor) by calmodulin. *Biochem Biophys Res Commun* **213**, 1082–1090.
102 Tripathy A, Xu L, Mann G & Meissner G (1995) Calmodulin activation and inhibition of skeletal muscle Ca2 + release channel (ryanodine receptor). *Biophys J* **69**, 106–119.
103 Balshaw DM, Xu L, Yamaguchi N, Pasek DA & Meissner G (2001) Calmodulin binding and inhibition of cardiac muscle calcium release channel (ryanodine receptor). *J Biol Chem* **276**, 20144–20153.
104 Yamaguchi N, Xu L, Pasek DA, Evans KE & Meissner G (2003) Molecular basis of calmodulin binding to cardiac muscle Ca(2 +) release channel (ryanodine receptor). *J Biol Chem* **278**, 23480–23486.
105 Most P, Remppis A, Pleger ST, Loffler E, Ehlermann P, Bernotat J, Kleuss C, Heierhorst J, Ruiz P, Witt H *et al.* (2003) Transgenic overexpression of the Ca2 + -binding protein S100A1 in the heart leads to increased *in vivo* myocardial contractile performance. *J Biol Chem* **278**, 33809–33817.
106 Prosser BL, Wright NT, Hernandez-Ochoa EO, Varney KM, Liu Y, Olojo RO, Zimmer DB, Weber DJ & Schneider MF (2008) S100A1 binds to the calmodulin-binding site of ryanodine receptor and modulates skeletal muscle excitation–contraction coupling. *J Biol Chem* **283**, 5046–5057.
107 Maximciuc AA, Putkey JA, Shamoo Y & Mackenzie KR (2006) Complex of calmodulin with a ryanodine receptor target reveals a novel, flexible binding mode. *Structure* **14**, 1547–1556.
108 Wright NT, Prosser BL, Varney KM, Zimmer DB, Schneider MF & Weber DJ (2008) S100A1 and calmodulin compete for the same binding site on ryanodine receptor. *J Biol Chem* **283**, 26676–26683.

109 Prosser BL, Hernandez-Ochoa EO & Schneider MF (2011) S100A1 and calmodulin regulation of ryanodine receptor in striated muscle. *Cell Calcium* **50**, 323–331.
110 Amador FJ, Liu S, Ishiyama N, Plevin MJ, Wilson A, MacLennan DH & Ikura M (2009) Crystal structure of type I ryanodine receptor amino-terminal β-trefoil domain reveals a disease-associated mutation 'hot spot' loop. *Proc Natl Acad Sci USA* **106**, 11040–11044.
111 Lobo PA & Van Petegem F (2009) Crystal structures of the N-terminal domains of cardiac and skeletal muscle ryanodine receptors: insights into disease mutations. *Structure* **17**, 1505–1514.
112 Lobo PA, Kimlicka L, Tung CC & Van Petegem F (2011) The deletion of exon 3 in the cardiac ryanodine receptor is rescued by beta strand switching. *Structure* **19**, 790–798.
113 Sharma P, Ishiyama N, Nair U, Li W, Dong A, Miyake T, Wilson A, Ryan T, Maclennan DH, Kislinger T *et al.* (2012) Structural determination of the phosphorylation domain of the ryanodine receptor. *FEBS J* **279**, 3952–3964.
114 Yuchi Z, Lau K & Van Petegem F (2012) Disease mutations in the ryanodine receptor central region: crystal structures of a phosphorylation hot spot domain. *Structure* **20**, 1201–1211.
115 White RR, Kwon YG, Taing M, Lawrence DS & Edelman AM (1998) Definition of optimal substrate recognition motifs of Ca2 + -calmodulin-dependent protein kinases IV and II reveals shared and distinctive features. *J Biol Chem* **273**, 3166–3172.
116 Ponting C, Schultz J & Bork P (1997) SPRY domains in ryanodine receptors (Ca(2 +)-release channels). *Trends Biochem Sci* **22**, 193–194.
117 Tae H, Casarotto MG & Dulhunty AF (2009) Ubiquitous SPRY domains and their role in the skeletal type ryanodine receptor. *Eur Biophys J* **39**, 51–59.
118 Casarotto MG, Cui Y, Karunasekara Y, Harvey PJ, Norris N, Board PG & Dulhunty AF (2006) Structural and functional characterization of interactions between the dihydropyridine receptor II–III loop and the ryanodine receptor. *Clin Exp Pharmacol Physiol* **33**, 1114–1117.
119 Kimura T, Pace SM, Wei L, Beard NA, Dirksen RT & Dulhunty AF (2007) A variably spliced region in the type 1 ryanodine receptor may participate in an inter-domain interaction. *Biochem J* **401**, 317–324.
120 Cui Y, Tae HS, Norris NC, Karunasekara Y, Pouliquin P, Board PG, Dulhunty AF & Casarotto MG (2009) A dihydropyridine receptor alpha1s loop region critical for skeletal muscle contraction is intrinsically unstructured and binds to a SPRY domain of the type 1 ryanodine receptor. *Int J Biochem Cell Biol* **41**, 677–686.
121 Tae HS, Cui Y, Karunasekara Y, Board PG, Dulhunty AF & Casarotto MG (2011) Cyclization of the intrinsically disordered alpha1S dihydropyridine receptor II–III loop enhances secondary structure and *in vitro* function. *J Biol Chem* **286**, 22589–22599.
122 Dulhunty AF, Karunasekara Y, Curtis SM, Harvey PJ, Board PG & Casarotto MG (2005) The recombinant dihydropyridine receptor II–III loop and partly structured 'C' region peptides modify cardiac ryanodine receptor activity. *Biochem J* **385**, 803–813.
123 Lu X, Xu L & Meissner G (1994) Activation of the skeletal muscle calcium release channel by a cytoplasmic loop of the dihydropyridine receptor. *J Biol Chem* **269**, 6511–6516.
124 Stange M, Tripathy A & Meissner G (2001) Two domains in dihydropyridine receptor activate the skeletal muscle Ca(2 +) release channel. *Biophys J* **81**, 1419–1429.
125 Rebbeck RT, Karunasekara Y, Gallant EM, Board PG, Beard NA, Casarotto MG & Dulhunty AF (2011) The beta(1a) subunit of the skeletal DHPR binds to skeletal RyR1 and activates the channel via its 35-residue C-terminal tail. *Biophys J* **100**, 922–930.
126 Sheridan DC, Cheng W, Carbonneau L, Ahern CA & Coronado R (2004) Involvement of a heptad repeat in the carboxyl terminus of the dihydropyridine receptor beta1a subunit in the mechanism of excitation–contraction coupling in skeletal muscle. *Biophys J* **87**, 929–942.
127 Neuhuber B, Gerster U, Doring F, Glossmann H, Tanabe T & Flucher BE (1998) Association of calcium channel alpha1S and beta1a subunits is required for the targeting of beta1a but not of alpha1S into skeletal muscle triads. *Proc Natl Acad Sci USA* **95**, 5015–5020.
128 Leuranguer V, Papadopoulos S & Beam KG (2006) Organization of calcium channel beta1a subunits in triad junctions in skeletal muscle. *J Biol Chem* **281**, 3521–3527.
129 Radermacher M, Rao V, Grassucci R, Frank J, Timerman AP, Fleischer S & Wagenknecht T (1994) Cryo-electron microscopy and three-dimensional reconstruction of the calcium release channel/ryanodine receptor from skeletal muscle. *J Cell Biol* **127**, 411–423.
130 Serysheva II, Orlova EV, Chiu W, Sherman MB, Hamilton SL & van Heel M (1995) Electron cryomicroscopy and angular reconstitution used to visualize the skeletal muscle calcium release channel. *Nat Struct Biol* **2**, 18–24.
131 Ludtke SJ, Serysheva II, Hamilton SL & Chiu W (2005) The pore structure of the closed RyR1 channel. *Structure* **13**, 1203–1211.

132 Samso M, Wagenknecht T & Allen PD (2005) Internal structure and visualization of transmembrane domains of the RyR1 calcium release channel by cryo-EM. *Nat Struct Mol Biol* **12**, 539–544.
133 Serysheva II, Ludtke SJ, Baker ML, Cong Y, Topf M, Eramian D, Sali A, Hamilton SL & Chiu W (2008) Subnanometer-resolution electron cryomicroscopy-based domain models for the cytoplasmic region of skeletal muscle RyR channel. *Proc Natl Acad Sci USA* **105**, 9610–9615.
134 Samso M, Feng W, Pessah IN & Allen PD (2009) Coordinated movement of cytoplasmic and transmembrane domains of RyR1 upon gating. *PLoS Biol* **7**, e85.
135 Kimlicka L & Van Petegem F (2011) The structural biology of ryanodine receptors. *Sci China Life Sci* **54**, 712–724.
136 Raina SA, Tsai J, Samso M & Fessenden JD (2012) FRET-based localization of fluorescent protein insertions within the ryanodine receptor type 1. *PLoS One* **7**, e38594.
137 Meng X, Xiao B, Cai S, Huang X, Li F, Bolstad J, Trujillo R, Airey J, Chen SR, Wagenknecht T *et al.* (2007) Three-dimensional localization of serine 2808, a phosphorylation site in cardiac ryanodine receptor. *J Biol Chem* **282**, 25929–25939.
138 Yin CC, D'Cruz LG & Lai FA (2008) Ryanodine receptor arrays: not just a pretty pattern? *Trends Cell Biol* **18**, 149–156.
139 Yin CC & Lai FA (2000) Intrinsic lattice formation by the ryanodine receptor calcium-release channel. *Nat Cell Biol* **2**, 669–671.
140 Ludtke SJ, Tran TP, Ngo QT, Moiseenkova-Bell VY, Chiu W & Serysheva II (2011) Flexible architecture of IP3R1 by cryo-EM. *Structure* **19**, 1192–1199.
141 Yuchi Z & Van Petegem F (2011) Common allosteric mechanisms between ryanodine and inositol-1,4,5-trisphosphate receptors. *Channels (Austin)* **5**, 120–123.
142 Mikoshiba K (2007) The IP3 receptor/Ca2+ channel and its cellular function. *Biochem Soc Symp* **74**, 9–22.
143 Boehning D & Joseph SK (2000) Direct association of ligand-binding and pore domains in homo- and heterotetrameric inositol 1,4,5-trisphosphate receptors. *EMBO J* **19**, 5450–5459.
144 Edgar RC (2004) MUSCLE: multiple sequence alignment with high accuracy and high throughput. *Nucleic Acids Res* **32**, 1792–1797.
145 Tamura K, Peterson D, Peterson N, Stecher G, Nei M & Kumar S (2011) MEGA5: molecular evolutionary genetics analysis using maximum likelihood, evolutionary distance, and maximum parsimony methods. *Mol Biol Evol* **28**, 2731–2739.